

Supporting Information for

Photocatalytic hydrogen production and storage in carbon
nanotubes: A first-principle study

Xiaohan Song^a, Hongxia Bu^b, Yingcai Fan^c, Junru Wang^d, Mingwen Zhao^{e*}

^a *Shandong Institute of Advanced Technology, Jinan, Shandong, 250100, China*

^b *College of Physics and Electronic Engineering, Qilu Normal University, Jinan, Shandong
250200, China*

^c *School of Information and Electronic Engineering, Shandong Technology and Business
University, Yantai, Shandong, 264005, China*

^d *Department of Physics, Yantai University, Yantai, Shandong, 264005, China*

^e *School of Physics and State Key Laboratory of Crystal Materials, Shandong University, Jinan,
Shandong, 250100, China*

Corresponding author, E-mail: zmw@sdu.edu.cn

Text S1. The strategy of NAMD calculation

The nonadiabatic molecular dynamics (NAMD) simulations were carried out by the Hefei-NAMD code, where the real-time time-dependent KS equation framework was used to model the photo-excited carrier relaxation¹. All structures were fully relaxed at 0 K, then we use the velocity rescaling to bring the temperature of the system to 100 K. After this, a 2.0 ps microcanonical ab initio molecular dynamics (MD) trajectory is then generated using a 1.0 fs time step. The NAMD results are based on an average over 100 different initial configurations obtained from the MD trajectory. For each chosen structure, we sample 2×10^4 trajectories for the last 1 ps.

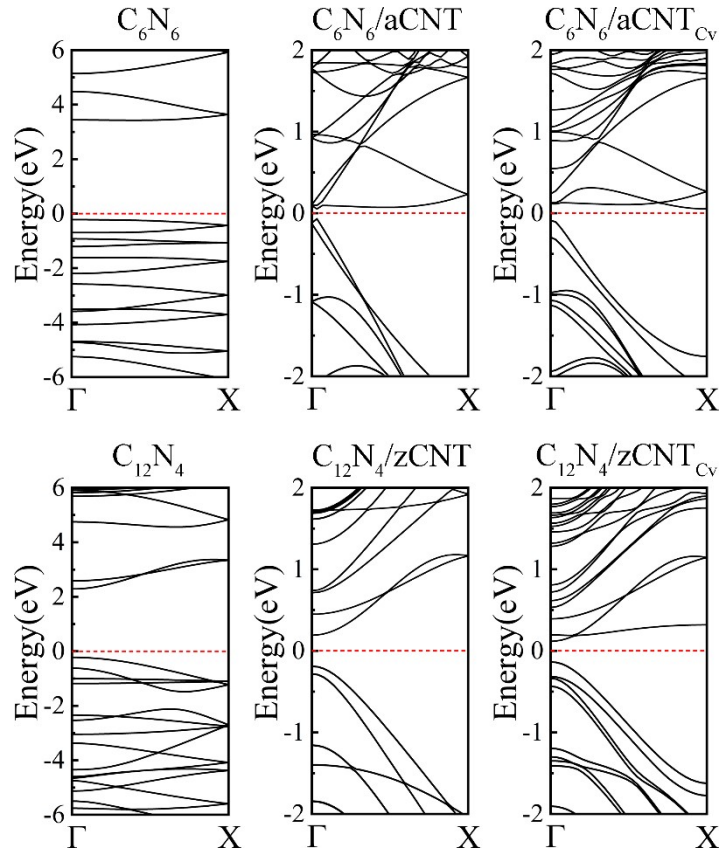


Fig. S1. Band structures of CNNWs (C_6N_6 and $C_{12}N_4$) and the core/shell structures ($C_6N_6/aCNT$, $C_{12}N_4/zCNT$, $C_6N_6/aCNT_{Cv}$ and $C_{12}N_4/zCNT_{Cv}$) calculated by using the HSE06 functional. The energy at the Fermi level was set to zero.

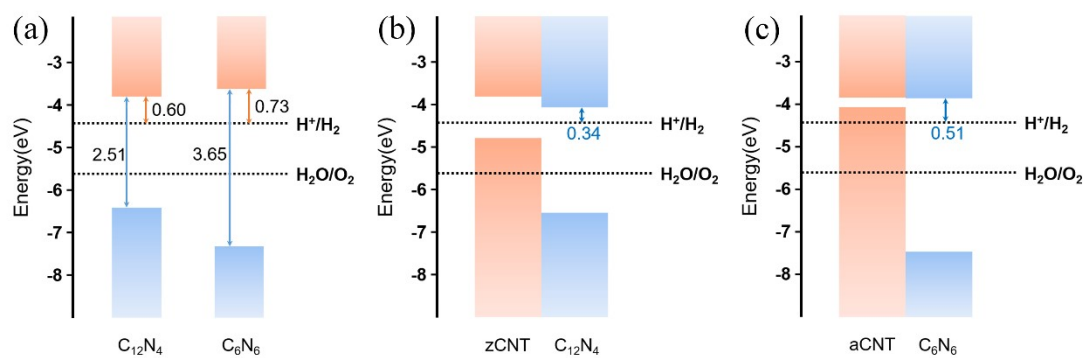


Fig. S2. Band edge alignment of (a) CNNWs (C_6N_6 and $C_{12}N_4$), (b) $C_{12}N_4/zCNT$ and (c) $C_6N_6/aCNT$ relative to the vacuum levels. The energy of the vacuum level was set to zero. The hydrogen reduction potential (H^+/H_2) and the water oxidation potential (H_2O/O_2) at pH 0 are -4.44 eV and -5.67 eV relative to the vacuum levels, respectively, which represented by the dotted lines.

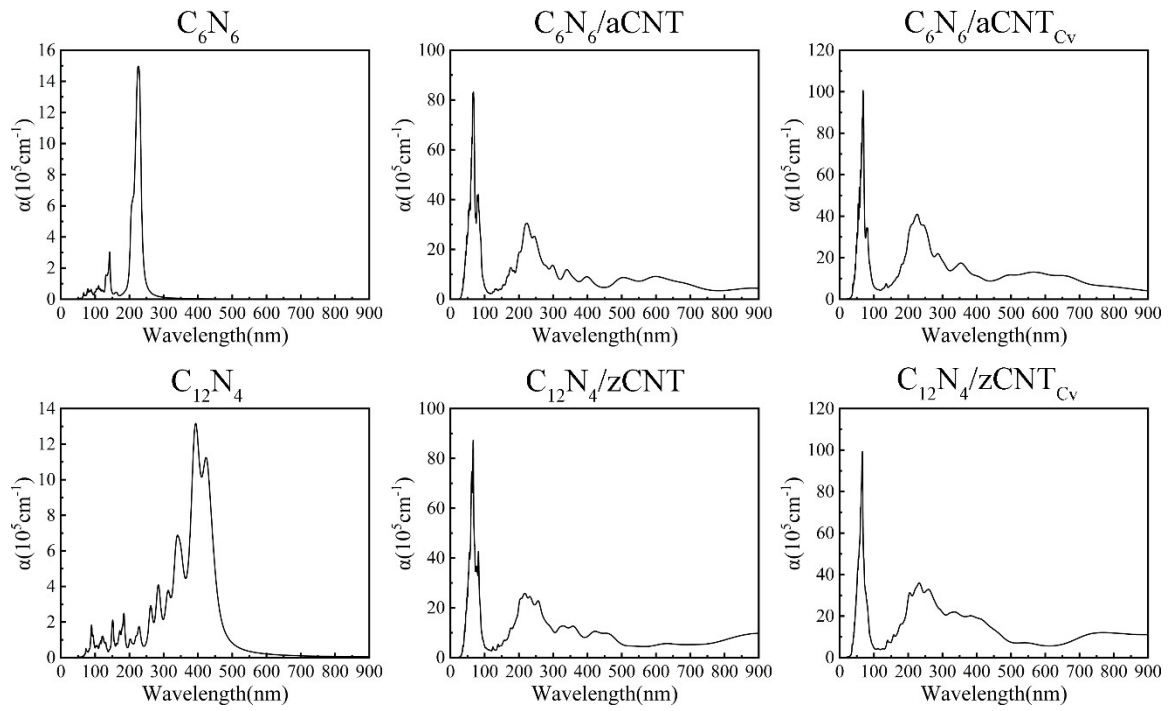


Fig. S3. Absorption coefficient of CNNWs (C_6N_6 and $C_{12}N_4$) and the core/shell structures ($C_6N_6/aCNT$, $C_{12}N_4/zCNT$, $C_6N_6/aCNT_{Cv}$ and $C_{12}N_4/zCNT_{Cv}$) calculated by using the HSE06 functional.

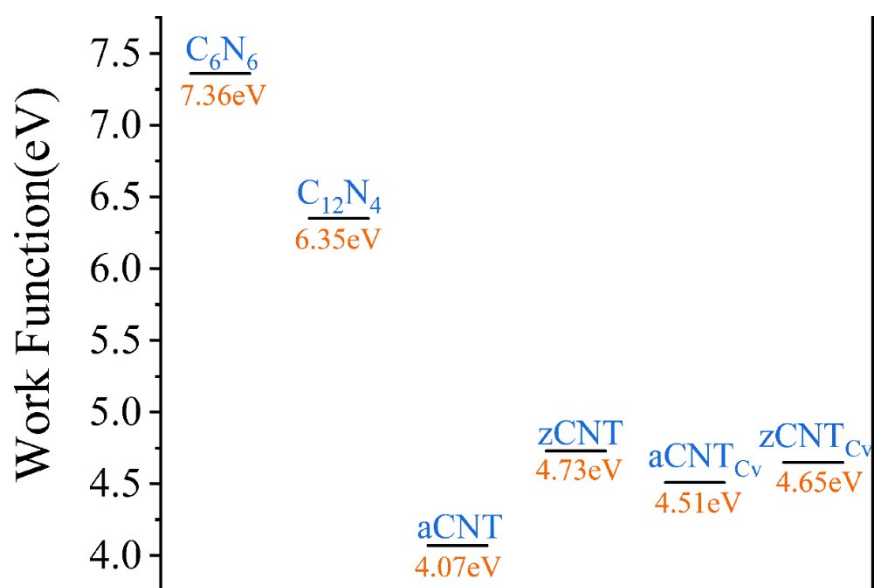


Fig. S4. The work functions of CNNWs (C_6N_6 and $C_{12}N_4$), CNTs (aCNT and zCNT) and CNTs with a vacancy (aCNT_{Cv} and zCNT_{Cv}) calculated by using the HSE06 functional.

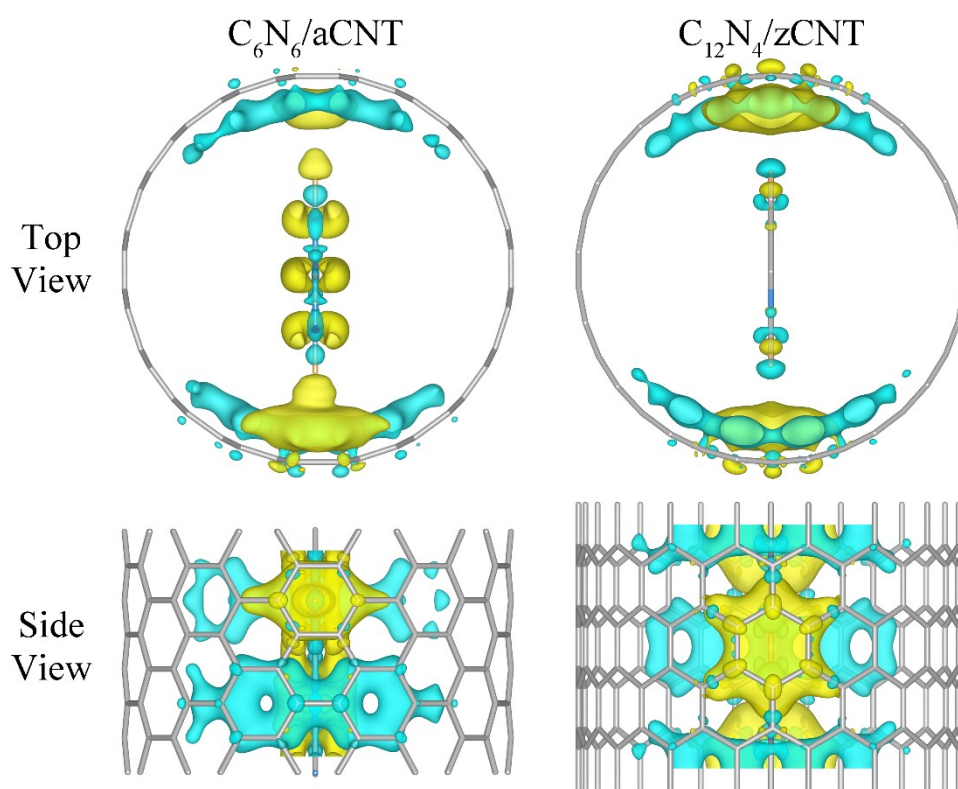


Fig. S5. Top and side views of charge density difference of the neutral core/shell structures ($C_6N_6/aCNT$ and $C_{12}N_4/zCNT$). The isosurfaces are $4 \times 10^{-4} e/\text{\AA}^3$. Yellow regions indicate electron accumulation, and blue regions indicate electron loss.

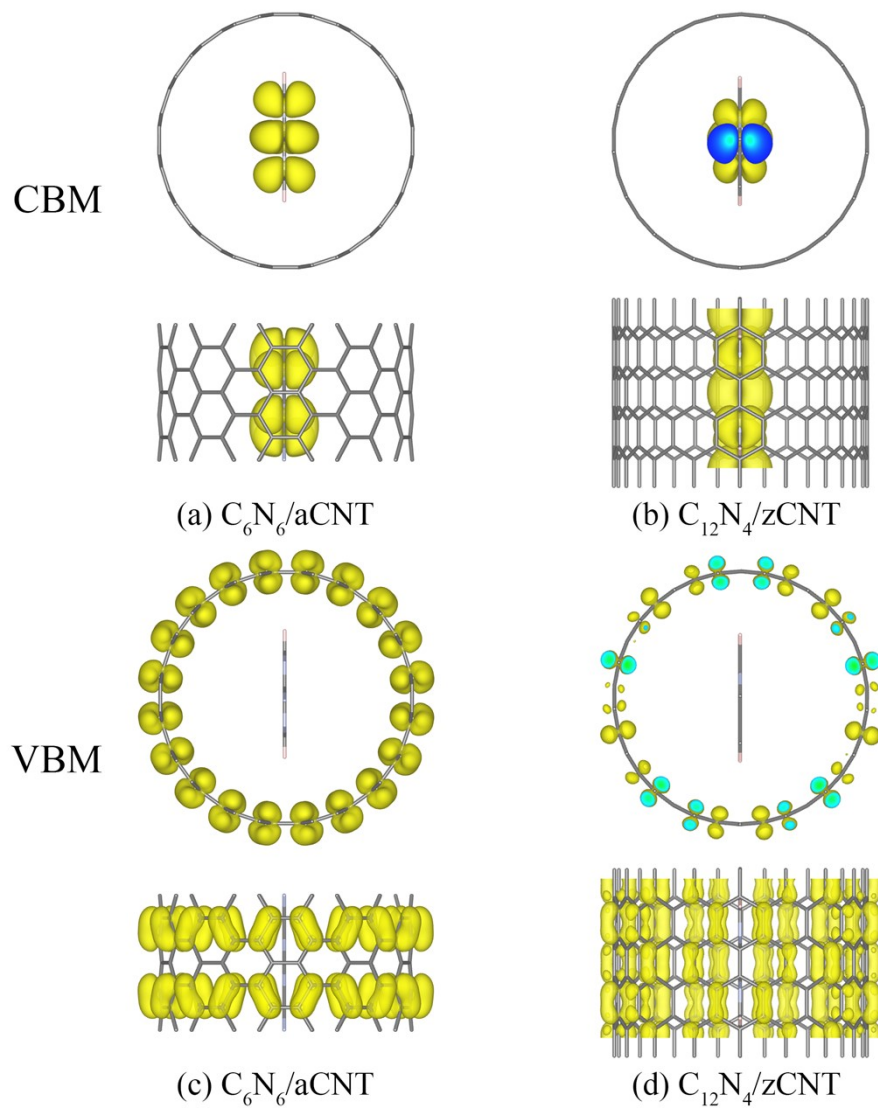


Fig. S6. Band-decomposed charge density distributions for the CBM and VBM of $C_6N_6/aCNT$ and $C_{12}N_4/zCNT$ structures. Yellow bubbles represent electron density with isosurface value of $3 \times 10^{-3} e/\text{\AA}^3$ and $1 \times 10^{-3} e/\text{\AA}^3$ respectively for $C_6N_6/aCNT$ and $C_{12}N_4/zCNT$ structures.

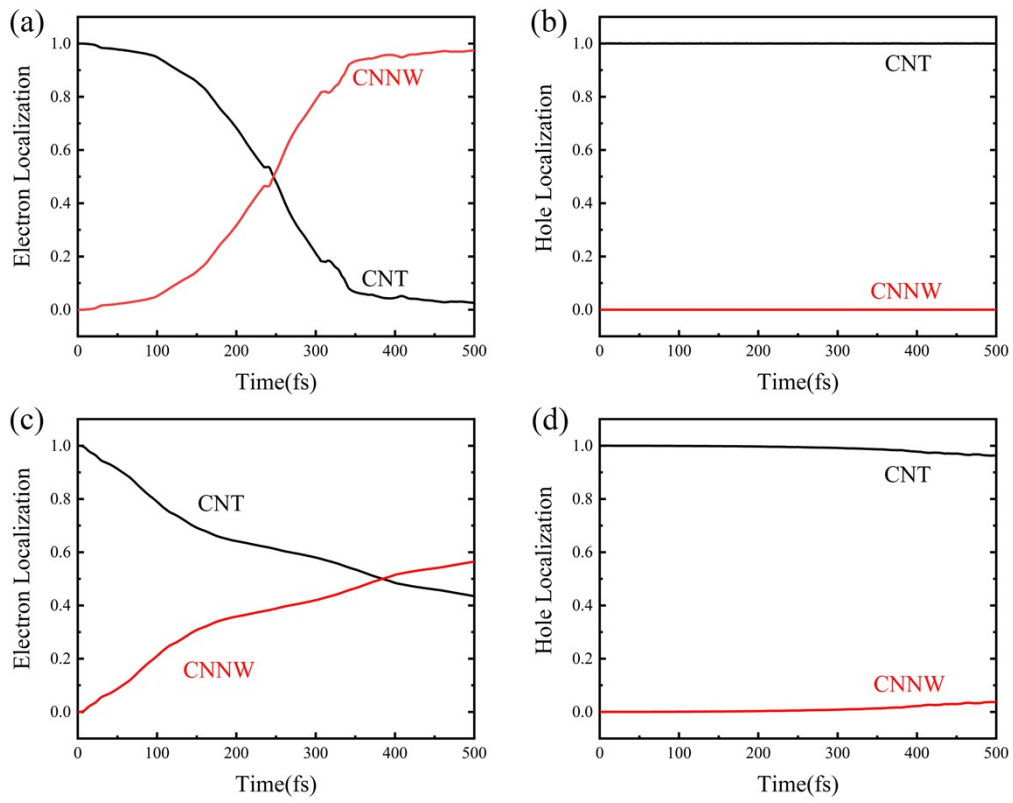


Fig. S7. The time dependent spatial charge localization of photogenerated (a) electron and (b) hole in the $C_6N_6/aCNT$ structure at 100 K. The time dependent spatial charge localization of photogenerated (c) electron and (d) hole in the $C_{12}N_4/zCNT$ structure at 100 K.

Table S1. Zero-point energy correction (E_{ZPE}) of the adsorbates considered in this work.

| $E_{\text{ZPE}}(\text{eV})$ | C_6N_6 | C_{12}N_4 |
|-----------------------------|------------------------|---------------------------|
| H^* | 0.324 | 0.328 |

References

1. Q. Zheng, W. Chu, C. Zhao, L. Zhang, H. Guo, Y. Wang, X. Jiang and J. Zhao, *Wiley Interdiscip. Rev.: Comput. Mol. Sci.*, 2019, **9**, e1411.